

VISUALIZATION OF STRATIFIED FLOWS AROUND A VERTICAL PLATE: LABORATORY EXPERIMENT AND NUMERICAL SIMULATION

YULI CHASHECHKIN¹ & YAROSLAV ZAGUMENNYI²

¹ Institute for Problems in Mechanics, Russian Academy of Sciences, Moscow, Russia.

² Institute of Hydromechanics, National Academy of Sciences of Ukraine, Kiev, Ukraine.

ABSTRACT

On the basis of the fundamental system, which includes equations of continuity, momentum, and substance transfer with a linearized equation of state, methods of experimental and numerical study are developed for visualizing the flow perturbation fields generated by uniform horizontal movement of a vertical plate in a stratified medium. The stratified flows were visualized in the laboratory tank by the high-sensitive and high-resolution Schlieren instrument IAB-458 at the stand ‘Laboratory Mobile Tank’ of the Unique Research Facility ‘HPC IPMech RAS’ and numerically calculated within the frame of the open source CFD utility OpenFOAM using computing resources of cluster systems and supercomputers. Both the computation results and the laboratory visualization data show that a vertical plate uniformly moving in a stratified fluid generates flow patterns which contain complex systems of internal waves, including upstream, attached and short ones, and thin interfaces, such as ligaments, formed due to the combined influence of the stratification and dissipation effects. Increase in the velocity of the plate movement leads to an essential restructuring of the wake flow past the plate, where typical vortex elements, such as vortex dipoles and ‘vortex bubbles’, are formed in the divergence zones of the phase surfaces of internal waves. All the flow structural components evolve and actively interact with each other and with the free stream. The observation and calculation results are in a good qualitative and quantitative agreement with each other.

Keywords: ligaments, OpenFOAM, stratified flow, vertical plate, vortices, visualization, waves.

1 INTRODUCTION

Studies of flows around a plate are a traditional object of experimental and theoretical investigations in hydro and aerodynamics due to the fundamental nature of the problem and the importance of practical applications. Starting from the first systematic studies carried out at the end of the 19th century, the flow pattern and the nature of the forces acting on an obstacle have been studied as functions of many parameters, including plate size, its angular position, density and free stream velocity of a fluid or a gas [1].

In the second half of the last century, due to the increasing interest in environmental fluid dynamics, the range of media types studied and factors taken into account was expanded, including numerical and experimental studies of the stratification effects naturally present in the environment [2]. Schlieren visualization images of flow patterns in the mode of intensive generation of attached internal waves by a cylinder and a vertical plate uniformly moving in a stratified fluid are demonstrated by Chashechkin *et al.* [3]. Vertical profile of the horizontal velocity component of the upstream flow perturbation was visualized using a density marker formed by the wake past a vertically emerging gas bubble which retains uniform motion at Reynolds numbers, $Re < 200$, defined by the diameter of a bubble and its ascent rate. Flow fine structure around a plate at various angles of attack was studied by Chashechkin *et al.* [4], though the principal attention of the article was focused at flow visualization around a horizontal plate and the methodological studies on the effects of the visualizing diaphragm shape on the features of a Schlieren image. Such an important detail of the flow pattern as the

presence of high-gradient interfaces was used for consistent optical and acoustic visualization of the flow past a vertical plate [5].

Calculations of the flow pattern past a vertical plate using turbulence models show a good qualitative and quantitative agreement with the observation data of internal wave patterns [6]; however, some fine structural elements, which are clearly observed in the experiments, are not visualized numerically due to the limitations of the problem formulation. Detailed experimental studies on the internal wave patterns generated by stratified flow past a thin barrier in a circular channel were also carried out by Sutherland and Linden [7]. The limited spatial resolution of the ‘synthetic Schlieren method’, which was used in this work, made it impossible to study the flow fine structure. Experimental data of the laboratory studies of the fine vortex wake structure past a vertical plate in a wind tunnel conducted by hot-wire anemometry are analyzed by Kiya and Matsumura [8].

Numerical simulation of laminar flow past a vertical plate was performed in by Castro *et al.* [9], and unsteady evolution of a weakly stratified flow was analyzed numerically in Chernyshenko and Castro [10] neglecting the influence of internal waves. During the recent years, mathematical models for flows around both solid and perforated plates have been created within the framework of modern versions of the turbulence theory in both the traditional two-dimensional formulation [11] and a more complete three-dimensional one [12]. A detailed numerical study on the incompressible homogeneous fluid flow around a solid and a porous vertical plate installed in a rectangular channel was carried out by Basnet and Constantinescu [13] using LES method. Patterns of streamlines and vorticity field visualizing the flow vortex structure, as well as calculations of forces and moments acting on an obstacle, are presented. Much attention is paid to comparison with the numerical studies by a lot of other authors. However, in contrast to the classical Schlieren visualization methods [3–5], computational techniques based on turbulence theory do not make it possible identifying the flow fine structure in inhomogeneous fluids and studying its effect on the flow dynamics.

The goal of the study is the development of consistent methods of laboratory modeling and numerical simulation of field patterns of observable physical variables in the problem on the flow around an obstacle moving in a uniformly stratified fluid. The system of fundamental equations of incompressible stratified fluid mechanics was chosen as a single basis for calculation methods and observation techniques, taking into account the dissipative factors, such as viscosity and diffusion effects, without involving additional hypotheses and parameters. Calculated fields of various physical quantities in the flow pattern around a vertical plate are presented, including the horizontal component of the density gradient field, which is experimentally visualized by Schlieren instruments with a Foucault knife.

2 GOVERNING EQUATIONS

Isothermal exponentially stratified fluid flows are considered in the uniform gravitational field with acceleration g . The stratification parameters are determined by values of the buoyancy scale, $\Lambda = |d \ln \rho / dz|^{-1}$, frequency, $N = \sqrt{g / \Lambda}$, and period, $T_b = 2\pi / N$, while the compressibility effects are neglected. The non-uniform density distribution, $\rho_0(z)$, is defined by the salinity profile, that is, the concentration of the solute, $S(z)$, which is assumed to be a linear function for a number of substances. This allows to write the state equation in the form, $\rho_0(z) = \rho_{00} S(z) = \rho_{00} (-z/\Lambda)$, where the salt compression coefficient is included in the definition of salinity.

The traditional system of equations for fluid mechanics taking into account the diffusion effects in the Boussinesq approximation takes the following form [14]:

$$\begin{aligned}
 \rho &= \rho_0 + \rho_{00} \cdot s, \quad \operatorname{div} \mathbf{v} = 0, \\
 \frac{\partial \mathbf{v}}{\partial t} + \nabla \cdot (\mathbf{v} \mathbf{v}) &= -\frac{1}{\rho_{00}} \nabla P + \nabla \cdot (\mathbf{v} \nabla \mathbf{v}) - s \cdot \mathbf{g}, \\
 \frac{\partial s}{\partial t} + \nabla \cdot (s \mathbf{v}) &= \nabla \cdot (\kappa_S \nabla s) + \frac{v_z}{\Lambda}.
 \end{aligned} \tag{1}$$

where ρ_{00} is the value of density on the reference level; $P(x, z, t)$ is the pressure except for the hydrostatic one; s is the salinity perturbation including the salt contraction coefficient; $\Lambda = |d \ln \rho / dz|^{-1}$, $N = \sqrt{g / \Lambda}$, and $T_b = 2\pi / N$ are the buoyancy scale, frequency and period, respectively; $\nu = 0.01 \text{ cm}^2/\text{s}$ and $\kappa_S = 1.41 \cdot 10^{-5} \text{ cm}^2/\text{s}$ are the kinematic viscosity and salt diffusion coefficients, respectively; t is time; and ∇ and Δ are the Hamilton and Laplace operators, respectively.

Physically valid no-slip and no-flux boundary conditions have the following form:

$$\begin{aligned}
 \mathbf{u}|_{t \leq 0} &= 0, \quad s|_{t \leq 0} = 0, \quad P|_{t \leq 0} = 0, \\
 \mathbf{u}_x|_{\Sigma} = \mathbf{u}_z|_{\Sigma} &= 0, \quad \left[\frac{\partial s}{\partial \mathbf{n}} \right]_{\Sigma} = \frac{1}{\Lambda} \frac{\partial z}{\partial \mathbf{n}}, \\
 \mathbf{u}_x|_{x, z \rightarrow \infty} &= U, \quad \mathbf{u}_z|_{x, z \rightarrow \infty} = 0.
 \end{aligned} \tag{2}$$

Such unsteady problems are usually solved in two stages. Initially, an obstacle under study is placed in a uniformly stratified fluid without external disturbances, which, in this particular case, is a vertical plate with height, h , length, L , and width W . Due to breaking the initial uniform density distribution, the plate generates specific fine-structured diffusion-induced flows, which were numerically studied in detail in Zagumennyi *et al.* [15]. However, since such flows are not formed on the vertical walls and these effects are rather weak for the case of a thin plate, their influence on the flow pattern can be neglected, and the problem on flow evolution can be solved immediately after the start of the body movement with a constant speed of U .

Construction of the computational programs and experimental techniques is based on the analysis of all the intrinsic structural components of the problem, including upstream perturbations, vortices, waves, and ligaments which are fine-structural components emerging due to the combined effects of dissipation and non-stationarity of the phenomenon under study [16].

The governing system of equations (1) together with the initial and boundary conditions (2) and the structural components of the flows under study are characterized by a set of temporal and spatial scales that are significantly different in values. Among the large linear scales are the buoyancy scale, $\Lambda = |d \ln \rho / dz|^{-1}$, which characterizes the manifestation level of the initial stratification, the geometric dimensions of the body, h, L, W , and the attached internal wavelength, $\lambda = UT_b$. Small scales characterizing ligaments [16] are determined by the dissipative properties of the medium by the kinetic coefficients of kinematic viscosity, ν , and diffusion of the stratifying component, κ_S , and the buoyancy frequency, $\delta_N^v = \sqrt{\nu / N}$ and $\delta_N^{\kappa_S} = \sqrt{\kappa_S / N}$, or the velocity of the body movement, which forms the flow under study, $\delta_U^v = \nu / N$ and $\delta_U^{\kappa_S} = \kappa_S / U$. A large number of intrinsic structural flow components with non-multiple, in a general case, intrinsic scales indicate non-stationarity of the phenomena under study.

The intrinsic time scales of the problem include the buoyancy period, T_b , the motion, $T_o = L/U$, and the fine structure parameters, such as viscous, $\tau_U^v = \nu/U^2$, and diffusion ones, $\tau_U^{k_s} = \kappa_s/U^2$.

The intrinsic scales define basic requirements for the experimental and numerical methods. The large linear scales, h, L, λ , determine the general dimensions of the tank or computational domain, which should contain a sufficient number of the flow components under study. The small ones, δ_N^v and $\delta_N^{k_s}$, define both spatial resolutions of the experimental instruments and computational mesh fineness in the numerical simulation. The typical time scales determine the requirements for numerical programs and experimental techniques. The large scales define the duration of the observation time, $T_o = L/U$, and small scales, $\tau_U^v, \tau_U^{k_s}$, define the calculation time step in computational programs, as well as the holding time for photo and video recording of a flow pattern.

3 TECHNIQUE OF LABORATORY EXPERIMENT

The laboratory experiments were conducted at the stand ‘Laboratory Mobile Tank (LMT)’, which is a part of the Unique Research Facility ‘Hydrophysical Complex of the IPMech RAS’ (HPC IPMech RAS) for modeling hydrodynamic processes in the environment and their impact on underwater technical objects, as well as distribution of impurities in the ocean and atmosphere (HPC IPMech) [17], designed to study the consistent optical, acoustic, and contact methods of dynamics and fine structure of two-dimensional (2D) and three-dimensional (3D) jets, wake flows, vortices, and internal waves in stratified and homogeneous fluids. The LMT stand, which is shown in Fig. 1, includes a transparent tank with dimensions of 2.20×0.40×0.60 m, three pairs of optical glass portholes mounted into its sidewalls, a system for creating and controlling fluid stratification, two drives for towing models, a carriage for installing and moving sensors, a sonar system, surface and internal wave transmitters, a mirror Schlieren device with Maksutov’s meniscus of IAB-458 type, a unit for controlling and collecting experimental data.

The working environment is water and stratified aqueous solution of common salt. The tank was filled with continuously stratified fluid from the bottom by the method of continuous displacement. In the experiments, a linear stratification was produced with buoyancy periods,

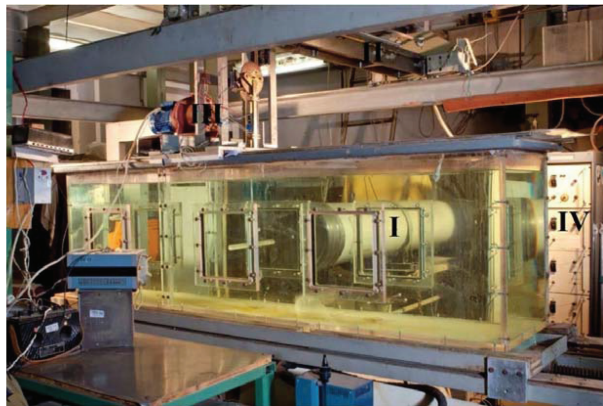


Figure 1: Laboratory Mobile Tank stand with Schlieren instrument IAB-458, including receiving part (I), carriage (II), wave producer (III), and control unit (IV).

$T_b = 2\pi/N = 7.5; 12.5; 17.4$ s, which correspond to values of buoyancy frequency, $N = \sqrt{g/\Lambda} = 0.84; 0.50; 0.35$ s⁻¹.

A flow pattern was observed using the IAB-458 Schlieren instrument with a 23 cm diameter field of view and spatial resolution less than 0.05 mm. As a lighting aperture, a vertical slit was used with a height of 10 mm and a width of 0.2 mm, and a flat vertical Foucault knife or Maksutov's thread was used as a receiving slit [18].

The working model is a rectangular plate with sharp edges made of stainless steel 2.5 cm in height, 39.5 cm in width and 2.0 mm in length (thickness). The plate was hanged on transparent knives to the carriage, which moved along guides mounted above the tank. The horizontal position of the plate edges and the trajectory of its movement were carefully controlled during the process of tank filling with respect to the free surface. The facility enables uniform movement of the plate at the center of the field of view along the longitudinal axis of the tank with velocities, $0.00 < U < 5.0$ in the range of significant influence of the buoyancy effects. At the start of each experiment, after filling the tank and decaying of all fine perturbations in the fluid, overall homogeneity of the stratification pattern was determined by the optical method, and buoyancy period was registered by means of a marker and a conductivity sensor with an error not exceeding 5%. As an extended vertical marker, the wake past a vertically emerging small gas bubble ($Re < 200$), or a freely immersing salt or sugar crystal, was observed by the Schlieren visualization method for a time period more than $16T_b$. In a series of experiments on marker deformation, the vertical distribution of the horizontal velocity component was measured [6].

In the present study, the experiments were conducted using a vertical slit illumination diaphragm and a flat vertical Foucault knife. Changes in illumination are proportional to variations in the horizontal component of the refraction index gradient. The refraction index, salinity, and density are related by linear ratios for the aqueous sodium chloride solution which was used to create the stratification. The coloring is due to the pronounced light dispersion in such a medium [19].

4 METHOD OF NUMERICAL SIMULATION

Numerical simulation of the governing equations (1) with the boundary conditions (2) is constructed using original C++ program codes of own development based on the finite volume method within the framework of the open-source computational utility OpenFOAM. Within the frame of the utility, a new solver was developed on the basis of the standard ones, used for solving Navier–Stokes equations for homogeneous viscous fluid, by supplementing them with additional equations for calculating fluid density and salinity, and specific program codes implementing no-flux boundary conditions for salinity perturbation on the impermeable surface of an obstacle under consideration.

The convective terms and time derivatives in the governing equations are interpolated with a limited TVD-scheme and the second-order implicit asymmetric three-point scheme with backward differencing, respectively. For solving the resultant system of linear equations, the conjugate (PCG) and biconjugate (PBiCG) gradient solvers are used together with DIC and DILU preconditioning for symmetric and asymmetric matrices, respectively. An iterative procedure for pressure–velocity coupling is implemented using the merged PISO-SIMPLE (PIMPLE) algorithm which has proven its high efficiency for unsteady flows [20].

The computation domain is discretized by a block-structured mesh with a high grading arranged toward the surface of a body in order to adequately take into account the viscous and diffusion effects in the near-wall region and provide an adequate resolution of the finest

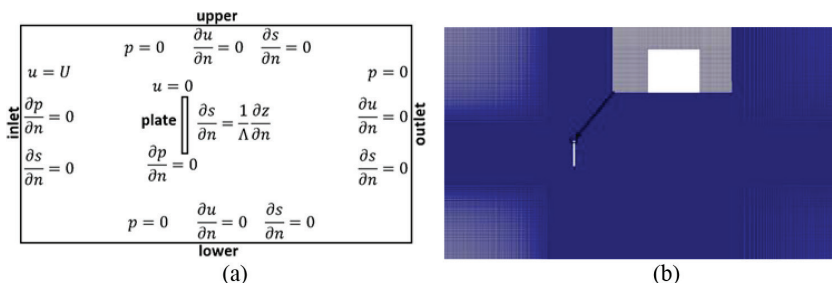


Figure 2: Draft of the computational domain (a) and a view of the mesh generated (b).

flow elements in the most perturbed flow region around the body [16]. Evaluations of minimal dimensions of the computational domain were based on a series of numerical experiments and were based on a criterion of the least disturbing effect of the free stream conditions specified at the outer boundaries on the flow structure. Particularly for the present numerical simulation, the optimal dimensions of the computational domain in the horizontal and vertical directions are of about 10 and 5 cm length of a body, respectively. In order to satisfy all the mentioned conditions for the numerical simulation, the total number of computational cells for the 2D case under consideration is about 2×10^6 . Draft of the computational domain with an indication of boundary conditions specified at all the boundaries (a) and a general view of the mesh generated with its detailed fragment around the plate corners are shown in Fig. 2.

The relatively high spatial and temporal resolution of the numerical model constructed as a result of satisfying the condition for adequate resolution of the finest flow components associated with the stratification and diffusion effects [16] makes it irrational performing calculations on personal computers due to a long computational time. So, the computations were carried out in parallel using the equipment of the shared research facilities of HPC computing resources at Lomonosov Moscow State University (<https://parallel.ru>) and the computing resources of the federal collective usage center Complex for Simulation and Data Processing for Mega-Science Facilities at NRC ‘Kurchatov Institute’ (<http://ckp.nrcki.ru>).

5 COMPUTATION RESULTS

In the calculated patterns of various physical fields around a vertical plate, including velocity, density perturbation, and density gradient, all the structural elements of the stratified flow, such as upstream perturbations, internal waves, and vortex wake past the obstacle, are well manifested (Fig. 3). However, there are noticeable differences in structural details and positions of high-gradient interfaces in patterns of the fields mentioned that demonstrates the functional independence of different physical variables.

The field of vertical velocity component has the simplest structure, which contains horizontal and oblique bands corresponding to a partially blocked fluid in front of the body and unsteady upstream internal waves above and below the plate’s edges. Past the body, the phase surfaces of the attached internal waves are closed into ligaments, such a set of high-gradient wake shells, which contact with the rear plane of the plate at a distance of 0.8 cm from its edges. The vertical size of the blocking zone in front of the plate is about 1.5 times smaller than the plate’s height that can be explained by a substantial influence of the stratification effects on the flow features in the vicinity of the obstacle. The outer part of the blocking zone is filled with the extended rays of unsteady half-wave, namely, a trough in the upper part and a crest in the lower one. The system of attached waves past the body is presented in Fig. 3a

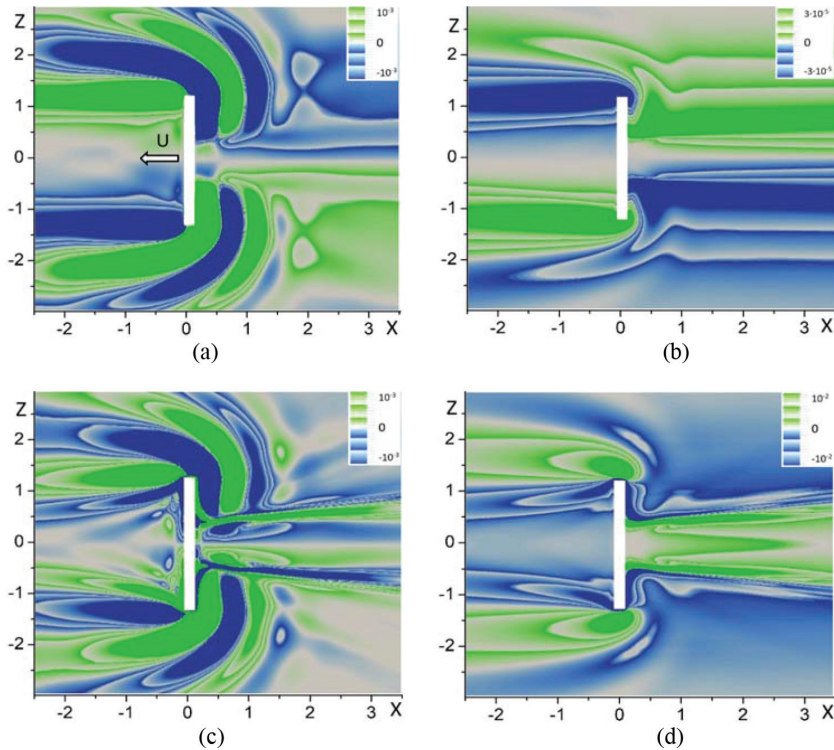


Figure 3: Calculated flow fields around a vertical plate. (a) Vertical component of velocity; (b) density perturbation; (c) horizontal, and (d) vertical components of density gradient; $h=2.5$ cm, $T_b=12.5$ s, $U=0.03$ cm/s.

by a sequence of curved bands with their outer part being composed of circular arcs which are smoothly transformed into the oblique rays of the upstream internal waves. The lower edges of the waves are in contact with the shells of the wake which expands in the vicinity of the crest and the trough in the upper and the lower half-spaces, respectively. And, on the contrary, in a half-wave, the distance between the marginal ligaments is minimal in the contacting area of the wave trough in the upper half-space. The attached internal wavelength, calculated in the frame of the linear theory, $\lambda = UT_b = 0.375$ cm, is in a good agreement with the observable value. The height of the wake flow smoothly increases with distance from the body.

The initial distribution of the density field is preserved in the center of the upstream perturbations with a wedge-shaped form (Fig. 3b). The height of the contacting area with the front surface of the plate is 1.4 cm, which is somewhat less than that for the velocity field in Fig. 3a. The unperturbed density field is also preserved in the vicinity of the central plane of the wake flow past the body. The thin ligaments limiting the wake at a distance of 0.65 cm from the plate are split into an elongated system of layered perturbations. The height of the contacting area of the ligaments with the rear surface is 0.75 cm, which is noticeably greater than that for the vertical velocity component field.

The most complex structural elements are observed in the field of the horizontal component of the density gradient (Fig. 3c). Here, wedge-shaped structures in the area of blocked fluid and fine-scale perturbations near the plate surface are clearly pronounced. Oblique ligaments bounding the wake flow past the body are split in the vicinity of the surface. The

height of the contact area is about 0.6 cm, which is comparable with the data for the velocity field and much larger than in the case of the density perturbation field. Phase surfaces in the form of internal wave rays in the vertical velocity component field are manifested in the most contrast. The system of weakly pronounced oblique bands in the right part of the figure visualizes the remains of the unsteady internal wave field arising as a result of the impulse start of the body movement, as it was also shown in the previous study [6].

The main perturbations in the vertical component of the density gradient field are concentrated in the upstream perturbation, and the shape of the ligaments reflects the internal wave field phase structure (Fig. 3d). The wedge-shaped contour of the density wake is wider in this field pattern, as compared with Fig. 3a–c, with an opening angle of about 25° and a minimum distance between the limiting ligaments of approximately 0.8 cm.

The attached internal waves become the most pronounced component of the flow structure at larger values of the plate velocity, $U=0.18$ cm/s, that is demonstrated by the calculated flow patterns in Fig. 4. In this case, the attached internal wavelength, $\lambda=2.25$ cm, is comparable with the plate's height, dissipative scales are $\delta_U^y = 0.05$ cm and $\delta_U^x = 6.6 \cdot 10^{-5}$ cm, and dimensionless numbers are $Re=45$ and $Fr=0.14$. Although under the new conditions, the upstream perturbations get less expressive, the main variations are observed in the flow region past the body. However, the blocking zone, where the fluid stays at rest for large distances from the plate surface, still remains clearly observable in the velocity field. A wedge-shaped region of the blocked fluid with a practically unperturbed density distribution adjacent to the rear side of the plate is contoured by oblique high-gradient interfaces (Fig. 4a). The high-gradient ligaments are mostly concentrated in the vicinity of the wake axis.

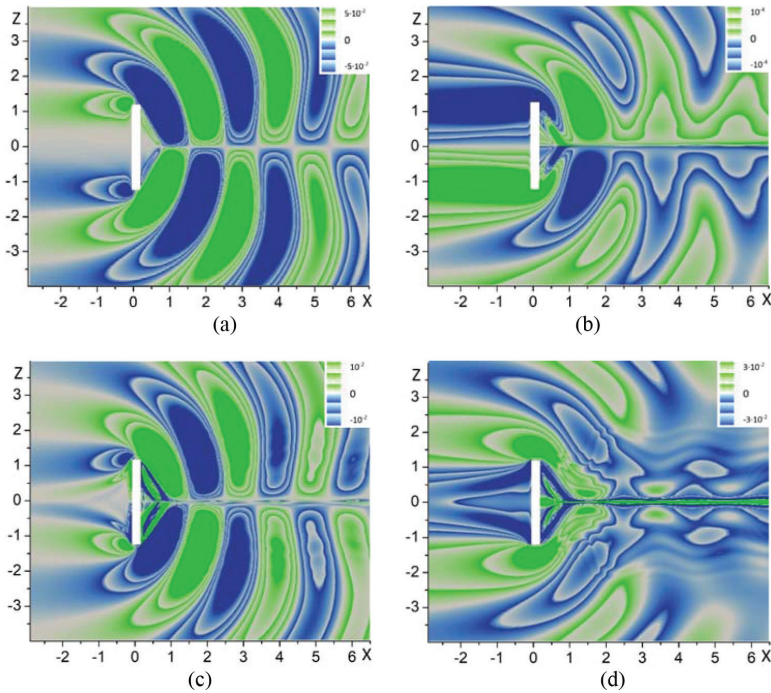


Figure 4: Calculated flow fields around a vertical plate. (a) Vertical component of velocity; (b) density perturbation; (c) horizontal, and (d) vertical components of density gradient; $h = 2.5$ cm, $T_b = 12.5$ s, $U = 0.18$ cm/s.

The wave perturbations in the density field decrease rapidly with distance from both the body and the wake axis (Fig. 4b). A narrow area of the blocked fluid in front of the plate is concentrated only in the vicinity of the flow axis. Most part of the blocking zone in front of the body is filled with zero-frequency internal waves. There are two visible groups of internal waves past the body, including attached ones with variable frequency and cylindrical-shaped phase surfaces, and standing ones with a frequency close to the buoyancy frequency in the vicinity of the central plane of the wake.

The overall pattern of the horizontal component of density gradient field is similar to the vertical velocity component field, but it exposes significantly finer details both in front of and past the body (Fig. 4c).

The wave perturbations in the pattern of the vertical component of density gradient field are manifested only in the vicinity of inclined line with maximum values of group velocity passing through the plate edges. The perturbations with positive values of the density gradient field in the blocking area are surrounded by two wedge-shaped areas with negative values, immersed into a system of unsteady upstream internal waves (Fig. 4d). A wedge-shaped region of bands with a lower intensity of perturbations adjoins to the rear part of the plate, which retains in the vicinity of the flow axis at a large distance from the body. The wake region is filled with systems of internal oscillations with the buoyancy frequency, being adjoined by extended linear perturbations with a typical waveform.

With the increase in the velocity of the plate movement, the attached internal waves grow in length, the flow pattern is saturated with new fine details, and the ligaments get clearer and smaller in scale (Fig. 5). Unsteady interaction between multiscale structural flow components

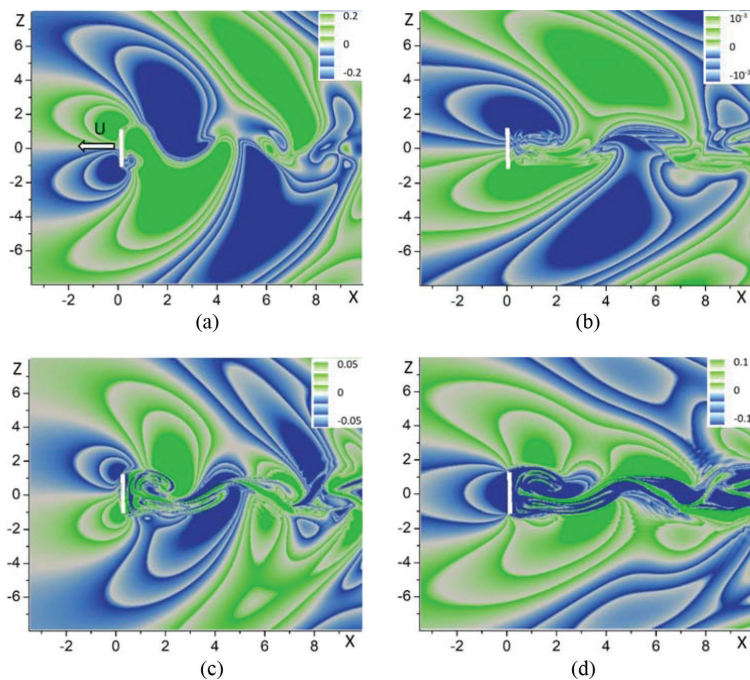


Figure 5: Calculated flow fields around a vertical plate. (a) Vertical component of velocity; (b) density perturbation; (c) horizontal, and (d) vertical components of density gradient; $h = 2.5$ cm, $T_b = 12.5$ s, $U = 0.75$ cm/s.

[21] leads to the emergence of new structural elements in the form of extended oscillating lines, as in Fig. 3d, and typical vortex structures which are clearly observed in Fig. 5. At the same time, within the range of Froude numbers, $Fr \leq 1.0$, there is a growth in the internal wave amplitude with an increase in the velocity of the plate movement.

In the velocity field pattern (Fig. 5a), the flow structure is predominated by several groups of wave perturbations, including relatively weak unsteady upstream waves in front of the body, short ones around the plate's edges, and long ones in the wake past the body where the waves are so strong that they distort the overall flow pattern, especially the central plane of the wake. In the wake flow, a set of spot-like wave perturbations with shorter wavelengths are also observed.

In the central part of the density field pattern in Fig. 5b, thin-layered ligaments are manifested, which separate the antiphase attached internal waves in the upper and lower half-spaces. They are traced throughout the whole wake, starting from the bottom side of the plate in the form of a wavy structure. The phase surfaces of the attached waves become oblique with their shape noticeably different from those previously calculated by the authors based on the linearized version of the system (1) or the complete non-linear formulation using one of the earlier RANS models for slightly different velocities of plate movement [6].

In the patterns of the density gradient fields shown in Fig. 5c and d, all the flow structural components, such as waves, ligaments, and compact vortices, are simultaneously represented. Two types of upstream internal waves are observed in front of the body, including longer ones coupled with the attached waves past the body and shorter ones localized at the plate's edges (Fig. 5d). In the vertical component of the density gradient field, only the long waves are manifested, which indicates the complexity of the spatial structure of the wave fields. The shape of the convoluted fine-structured wake with a vortex tip adjacent to the bottom part of the plate reflects the pattern of the attached waves in the flow regime under consideration. The overall flow pattern is unsteady with the bottom vortex forming a convoluted density wake by moving up and down along the surface of the plate.

6 COMPARISON

Comparison of the experimental data on high-resolution observations of the flow pattern, conducted by the Schlieren instrument IAB-458 at the LMT stand of the URF 'HPC IPMech RAS', shows a good qualitative and quantitative agreement with the calculations. The experiments were conducted using a vertical slit illumination diaphragm and a flat vertical Foucault knife. Changes in illumination are proportional to variations in the horizontal component of refraction index gradient which is in a linear relation to salinity and density gradients for the aqueous sodium chloride solution used to create the stratification.

The creeping flow regime at a slow body motion is characterized by existence of a set of flow structural components, including upstream oblique rays, internal waves attached past the body, and ligaments being formed at a distance from the plate edges and bounding the density wake (Fig. 6a)

In the regime of intense wave perturbations, both waves and an extensive family of ligaments forming a thin-layered wake are presented (Fig. 6b). Moreover, both in the calculations and the experiments, the upstream perturbation fine structure is visualized, indicating the existence of ligaments both past and in front of the body. In the experiments, the phase surfaces of the attached internal waves are deformed by the wake flow a bit stronger as compared with the calculation results, and the split pattern of thin-layered perturbations is more pronounced.

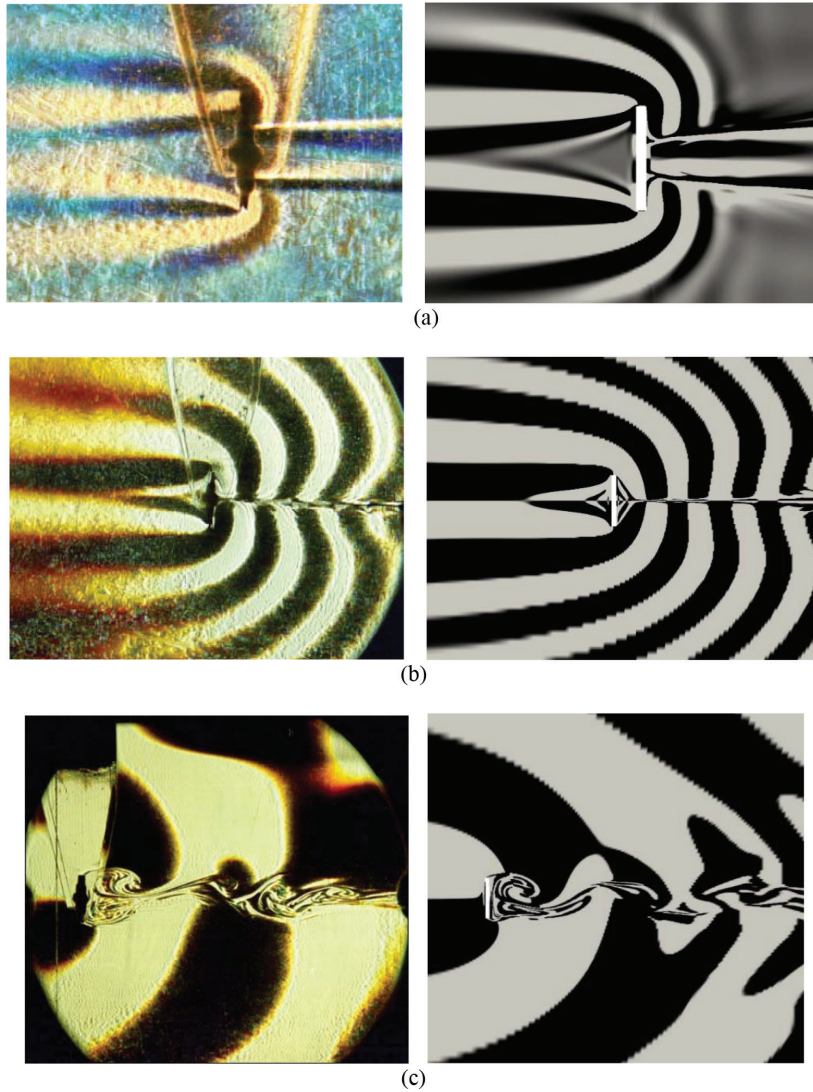


Figure 6: Comparison of Schlieren images (light refraction index gradient) and calculated flow patterns (horizontal component of density gradient) around a vertical plate uniformly moving in a continuously stratified fluid; $h = 2.5$ cm , $T_b = 12.5$ s ; (a) $U = 0.03$ cm/s ; (b) $U = 0.18$ cm/s ; (c) $U = 0.75$ cm/s.

With a further increase in the velocity, the general flow structure undergoes some modifications, such as leaning of the internal wavephase surfaces toward the direction of the body motion, and change in geometry of the fine-structural interfaces and manifestation degree of separate flow components (Fig. 6c). The strongest structural changes are observed in the wake past the plate, where typical vortex elements, such as vortex dipoles past the body and ‘vortex bubbles’, are formed in the divergence zones of the internal wave phase surfaces. All the flow components evolve and actively interact with each other and with the free stream. In

the unsteady flow regime, one can distinguish slowly evolving components, such as upstream and attached wave fields, rapidly changing ones, including fine-structured layers or ligaments, and their sets which are vortices.

7 CONCLUSIONS

Consistent experimental and theoretical studies of stratified flow dynamics and structure around a vertical plate are carried out based on the system of fundamental equations of incompressible stratified fluid mechanics, including the equations of continuity, Navier–Stokes and diffusion. The experimental technique and the computational program were developed taking into account the values of the intrinsic spatial and temporal scales of the problem that ensures visualization of the large-scale components, such as internal waves, and thin high-gradient interfaces or the so-called ligaments.

The stratified flows were experimentally visualized in the laboratory tank by the high-sensitive and high-resolution Schlieren instrument IAB-458 on the LMT stand of the URF ‘HPC IPMech RAS’. The numerical calculations were performed in parallel using computing resources of cluster systems and supercomputers based on original solvers of the open source CFD utility OpenFOAM.

Due to the scale invariance of the equations, the approach developed can be implemented in a wide range of parameters. However, in this article, the consideration was limited by uniform movement of a vertical plate with height, $h = 2.5$ cm, and speed of movement, $U = 0.003, 0.18$ and 0.75 cm/s, in a stratified fluid with buoyancy period $T_b = 12.5$ s. In the calculated patterns of the vertical velocity component, density perturbation, horizontal and vertical components of density gradient fields, systems of wake structures, unsteady and attached internal waves, and high-gradient interfaces (ligaments) are clearly distinguished. Along with a general structural similarity, the fine geometrical features of various physical fields are noticeably different for the same flow conditions.

At the smallest value of velocity of plate movement considered, the stratification substantially restricts the vertical size of the perturbations, so that the downstream wake contacts the rear side of the obstacle at some distance from its edges. With increase in the velocity, the vertical size of the wake grows and the contact area approaches the edges. At the highest value of velocity of plate movement considered, scale of the adjacent bottom vortex exceeds the plate’s height.

The program developed enables calculating other flow parameters, as well, in particular, pressure, streamlines, vorticity fields, baroclinic vorticity generation rate, mechanical energy dissipation rate, forces, and torques acting on an obstacle. On the basis of the fundamental system, which includes equations of continuity, momentum, and substance transfer with a linearized equation of state, methods of experimental and numerical study are developed for visualizing the flow perturbation fields generated by uniform movement of a vertical plate in a stratified medium.

Both in the calculated and visualized flow patterns formed by uniform movement of a vertical plate, systems of internal waves, including upstream, attached and short ones, and thin interfaces, such as ligaments, formed due to the combined influence of the stratification and dissipation effects, are distinguished.

The observation and calculation results are in a good qualitative and quantitative agreement with each other.

ACKNOWLEDGEMENTS

The experiments were conducted at the stand of the Unique Research Facility ‘Hydrophysical complex IPMech RAS (HPC IPMech RAS)’. The work was partially supported by the Ministry of Science and High Education within the framework of the Russian State Assignment under contract No. AAAA-A17-117021310378-8 ‘Development of coordinated analytical-numerical methods for calculating the dynamics and structure of fluid flows and comparison techniques with data of high-resolution experiments on the stands of the URF’ ‘HPC IPMech RAS’ and the RFBR Grant #18-05-00870’. The computations were performed using the equipment of the shared research facilities of HPC computing resources at Lomonosov Moscow State University and the computing resources of the Federal Collective Usage Center Complex for Simulation and Data Processing for Mega-Science Facilities at NRC ‘Kurchatov Institute’.

REFERENCES

- [1] Schlichting, H. & Gersten, K., *Boundary Layer Theory*, Springer-Verlag: Berlin, 2017.
- [2] Turner, J.C., *Buoyancy Effects in Fluids*, Cambridge University Press, 1973.
- [3] Chashechkin, Yu.D. & Mitkin, V.V., Experimental study of a fine structure of 2D wakes and mixing past an obstacle in a continuously stratified fluid. *Dynamics of Atmosphere and Oceans*, **34**, pp. 165–187, 2001.
- [4] Chashechkin, Yu.D. & Mitkin, V.V., A visual study on flow pattern around the strip moving uniformly in a continuously stratified fluid. *Journal of Visualization*, **7(2)**, pp. 127–134, 2004.
- [5] Prokhorov, V.E. & Chashechkin, Yu.D., Visualization and acoustic sounding of the fine structure of a stratified flow behind a vertical plate. *Fluid Dynamics*, **48(6)**, pp. 722–733, 2013.
- [6] Houcine, H., Chashechkin, Yu.D., Fraunie, Ph., Fernando, H., Gharbi, A. & Lili, T., Numerical modeling of the generation of internal waves by uniform stratified flow over a thin vertical barrier. *International Journal for Numerical Methods in Fluids*, **68**, pp. 451–466, 2012.
- [7] Sutherland, B.R. & Linden, P.F., Internal wave excitation from stratified flow over a thin barrier. *Journal of Fluid Mechanics*, **377**, pp. 223–252, 1998.
- [8] Kiya, M. & Matsumura, M., Incoherent turbulence structure in the near wake of a normal plate. *Journal of Fluid Mechanics*, **190**, pp. 343–356, 1988.
- [9] Castro, P., Cliffe, K.A. & Norgett, M.J., Numerical predictions of the laminar flow over a normal flat plate. *International Journal for Numerical Methods in Fluids*, **2**, pp. 61–88, 1982.
- [10] Chernyshenko, S.I. & Castro, I.P., High-Reynolds-number weakly stratified flow past an obstacle. *Journal of Fluid Mechanics*, **317**, pp. 155–178, 1996.
- [11] Castro, I.P., Wake characteristics of two-dimensional perforated plates normal to an air-stream. *Journal of Fluid Mechanics*, **46**, pp. 599–609, 1971.
- [12] Basnet, K. & Constantinescu, G., The structure of turbulent flow around vertical plates containing holes and attached to a channel bed. *Physics of Fluids*, **29(11)**, 115101, 2017.
- [13] Basnet, K. & Constantinescu, G., Effect of a bottom gap on the mean flow and turbulence structure past vertical solid and porous plates situated in the vicinity of a horizontal channel bed. *Physical Review Fluids*, **4**, 044604, 2019.

- [14] Landau, L.D. & Lifshits, E.M., *Theoretical Physics. Hydromechanics*. Pergamon Press, 1987.
- [15] Zagumennyi, Ia.V. & Chashechkin, Yu.D., Diffusion induced flow on a strip: Theoretical, numerical and laboratory modelling. *Procedia IUTAM*, **8**, pp. 256–266, 2013.
- [16] Chashechkin, Yu.D. & Zagumennyi, Ia.V., Formation of waves, vortices and ligaments in 2D stratified flows around obstacles. *Physica Scripta*, **94(5)**, 054003, 2019.
- [17] Hydrophysical Complex for Modeling Hydrodynamic Processes in the Environment and Their Impact on Underwater Technical Objects, as well as the Distribution of Impurities in the Ocean and Atmosphere, IPMech RAS, Online, <http://ipmnet.ru/uniquequip/gfk>
- [18] Maksutov, D.D., Shadow methods of analyzing optical systems. *Seriya Problemy Noveishei Fiziki*, **23**, GTI, 1934.
- [19] Chashechkin, Yu.D., Schlieren visualization of a stratified flow around a cylinder. *Journal of Visualization*, **1(4)**, pp. 345–354, 1999.
- [20] Jasak, H., OpenFOAM: Open source CFD in research and industry. *International Journal of Naval Architecture and Ocean Engineering*, **1(2)**, pp. 89–94, 2009.
- [21] Kistovich, Yu.V. & Chashechkin, Yu.D., A new mechanism of the non-linear generation of internal waves. *Doklady Physics*, **47(2)**, pp. 163–167, 2002.